

FLOW SIMULATION OVER A TWO-DIMENSIONAL MODEL HILL

Alexandru Cezar VLĂDUT¹, Radu Mircea DAMIAN², Mircea DEGERATU³,
Costin Ioan COȘOIU⁴, Andrei-Mugur GEORGESCU⁵

The paper presents the influence of different numerical models as well as of different input parameters for the evaluation of the flow in the simulated atmospheric boundary layer. One important aspect that was tested is the solver's ability to reproduce recirculation. We compared the numerical velocity distributions in ten vertical sections using different $k-\varepsilon$ models with the corresponding data from experiments and we obtained a good agreement. Then we have compared the turbulent kinetic energy distributions in the same sections. Furthermore, we performed a grid dependence and density test to determine the most economic grid that permits a similar result.

Keywords: flow, numerical simulation, boundary layer, hill

1. Introduction

In this article, we determined a robust turbulence model to be used for simulating the flow over simple terrain surfaces in the Atmospheric Boundary Layer (ABL) with low computational effort. This turbulence model is able to reproduce the complex flow patterns, which cannot be highlighted by conventional RANS models.

In order to determine the optimal turbulence model, we tried several $k-\varepsilon$ variants. The investigated turbulence models were used to perform numerical simulations on the flow over an obstacle with a 2D polynomial form, mounted on a flat plate which produces a recirculation region in the downstream region. The turbulence models were implemented in the ANSYS-Fluent expert software. Also, the simulations seek to identify the optimal characteristics of the computational grid.

The numerical simulations were reproducing the experimental set-up of the C18 test case from the European Research Community On Flow, Turbulence

¹ Assist. Prof., Hydraulics and Environmental Protection Department (HEPD), Technical University of Civil Engineering Bucharest, Romania, e-mail: cezar.vladut@utc.ro

² Prof., HEPD, Technical University of Civil Engineering Bucharest, radu.damian@aracis.ro

³ Prof., HEPD, Technical University of Civil Engineering Bucharest, mircead@hidraulica.utc.ro

⁴ Assoc. Prof., HEPD, Technical Univ. Civil Engineering Bucharest, costin@hidraulica.utc.ro

⁵ Prof., HEPD, Technical University of Civil Engineering Bucharest, andreig@hidraulica.utc.ro

And Combustion (ERCOFTAC) Classic Database on Manchester School of Mechanical, Aerospace and Civil Engineering website. This test case refers to a 2D-hill model mounted on the bottom of a channel on a flat plate with recirculation region in its wake. The experimental tests were conducted by Almeida et al. [1], [2] and the velocity and the resulted turbulent kinetic energy were determined using a Laser Doppler Anemometry technique in a fully developed turbulent channel flow. The channel height was $H = 170$ mm and the maximum height and length of the hill were $h_{max} = 28$ mm and $2R = 108$ mm, respectively (see Fig. 1).

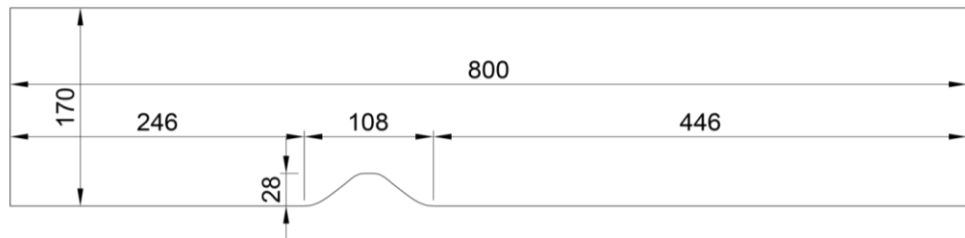


Fig. 1. 2D single hill flow: dimensions of the numerical simulation domain

2. Flow parameters

The experimental measurements were performed in a horizontal water tunnel with a length of 7 m, a width of 0.2 m and a height equal to H . As the flow may be considered identical in parallel vertical planes, the grid reproduces a part from a 2D longitudinal section trough the water tunnel. As mentioned in [1], the flow field is changed not just in the separation zone itself, but over the entire hill by the extent and strength of the recirculation zones established in the lee of the obstacle, so that defining the limits of the flow domain becomes a prerequisite of establishing the overall flow field. To achieve that, the boundaries must be appropriately located, far enough from the hill, so that the inflow and outflow boundaries have no spurious effects on the flow field around the hill and inside the recirculation area. Thus, the inlet section was placed at $8.79h_{max}$ upstream the hill, while the distance between the 2D-hill and the outlet section was equal to $15.92h_{max}$. Another interesting aspect that is somehow connected to the previous is the mean velocity speed-up which occurs on the hilltop ([3], [4]).

The fluid used in simulations was water with a kinematic viscosity $\nu = 1 \times 10^{-6}$ m²/s.

At the inlet section, a velocity profile was imposed, reproducing the experimental data, with the mean center line velocity equal to $U_o = 2.147$ m/s (see Fig. 2). The Reynolds number of the fully developed flow, computed with U_o and h_{max} is $Re = 60000$. [5][6].

At the inlet section, the turbulence intensity is about 3%, the friction factor is $C_f = 0.0027$ and the wall friction velocity is $\mu_r = 0.079$ m/s ([5], [6]).

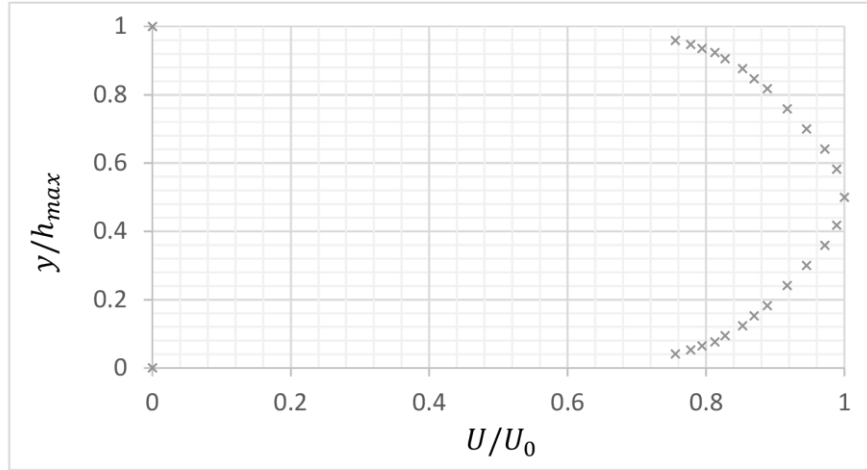


Fig. 2. The inlet profile

3. The turbulence models and the computational grid

Cabezon et al. [7] used different RANS models to investigate the flow around the Bolund island with promising results. A list with variants for the $k-\varepsilon$ turbulence model was created (see Table 1), considering also the proposed versions in [7]. Multiple numerical simulations were performed using the same grid and boundary conditions, varying only the turbulence model. Mesh refinements were carried out to ensure that the results are independent of the grid density. A reference grid was used in order to compare the different turbulence models' performances.

Table 1
The constants of different $k-\varepsilon$ turbulence model variants used in our simulations

$k-\varepsilon$ model	C_μ	$C_{l\varepsilon}$	$C_{2\varepsilon}$	σ_k	σ_ε
Standard	0.09	1.44	1.92	1.0	1.3
Realizable	0.09	1.44	1.9	1.0	1.2
RNG	0.0845	1.42	1.68	0.7194	0.7194
Monin-Obukhov	0.033	1.176	1.92	1.0	1.3
ABL model	0.0256	1.13	1.9	0.74	1.3

The meshes used in our simulations are structured, made from quad cells. If a grid mesh is chosen, the model must be able to accurately describe the flow at a low computational cost. Thus, the number of cells for the reference grid was kept low, equal to 26352, with 366 cells in the horizontal direction and 72 in the

vertical direction. Near the floor and at the upper part of the flow domain, the mesh was refined in order to capture better the velocity variation along the normal direction to the wall boundaries.

The gradients at the inflow and outflow boundaries are assumed to be zero. The errors caused by fluctuations at inflow should also be mitigated so that they do not influence the flow in the vicinity of the hill. That should be taken into consideration for the standard solution and, in order to be able to compare subsequent results with the standard solution, the same boundary conditions must be subsequently used.

4. Numerical tests results using the reference grid

The velocity and turbulent intensity distribution were compared in 13 transversal sections (see Fig. 3), corresponding to experimental vertical probing sections.

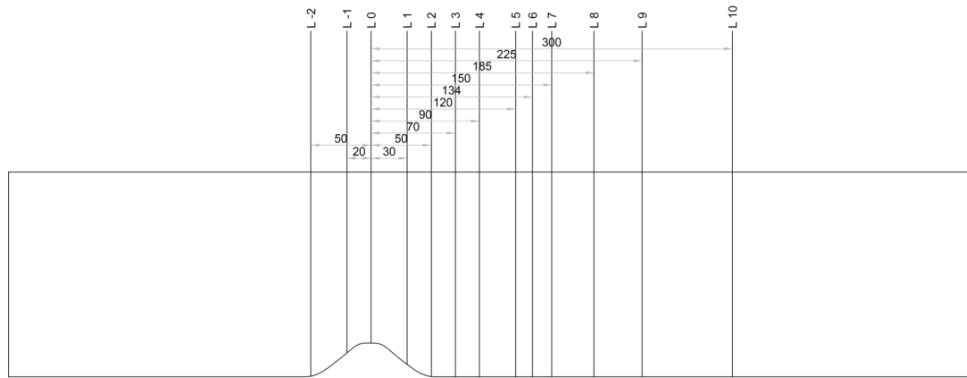


Fig. 3. Test sections used in comparison

Numerical tests have been carried out with different turbulence models. For the chosen 13 test sections, the computed dimensionless velocity distributions (U/U_0) depending on the dimensionless vertical coordinate (y/h_{max}) were compared with the distributions obtained experimentally (see Fig. 4). As one may observe, for sections L4 and L5, placed at the end of the recirculation zone. (Fig. 4) a good agreement was found between experiment and numerical simulations, especially for the $k-\varepsilon$ Monin-Obukhov and $k-\varepsilon$ ABL models.

However, as it can be seen in Figure 4 (gray areas are enlarged to make an easier comparison between numerical results and experimental results), this comparison was not conclusive for choosing a turbulent model that is the closest to the experimental measurements, so, next, we proceeded to compare the

turbulent kinetic energy distribution profiles in seven sections, were experimental data are provided.

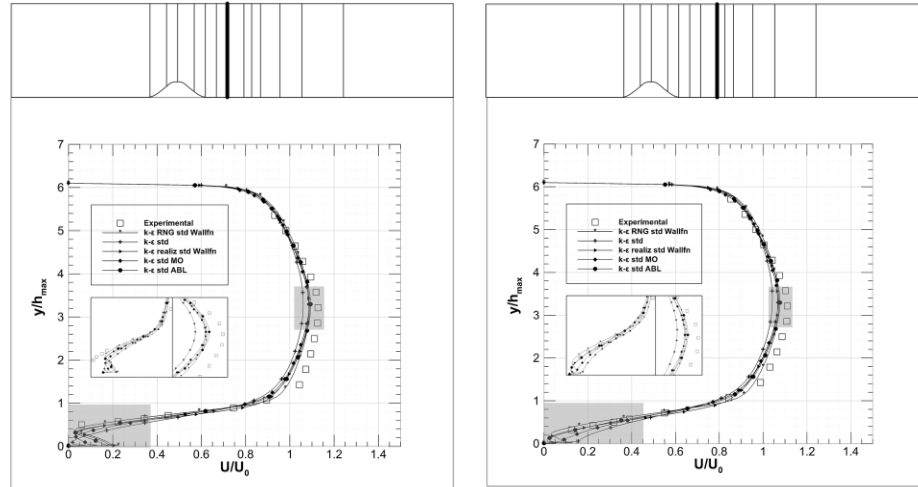


Fig. 4. Dimensionless velocity distributions U/U_0 depending on the vertical distance y/h_{max} for the five turbulence models compared with experimental distributions in section L4 and L5, downstream of the hill

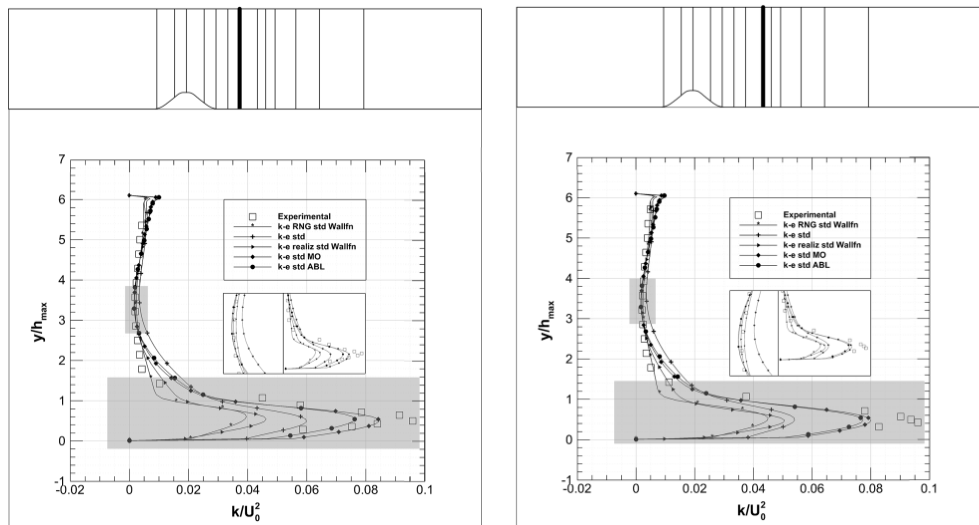


Fig. 5. Dimensionless turbulent kinetic energy distributions k/U_0^2 depending on the vertical distance y/h_{max} for the five turbulence models compared with experimental distributions in section L4 and L5, downstream of the hill

Further on, the computed vertical distributions of the dimensionless turbulent kinetic energy, k/U_0^2 , were compared with those obtained experimentally (Fig. 5).

When comparing the turbulent kinetic energy distributions, the turbulence models do not perform evenly. The prediction variation is high, with an error up to 60% for $k-\varepsilon$ RNG model.

Table 2 summarizes the test sections where the velocity and turbulent kinetic energy distributions obtained using numerical simulations closely agree with the experimental data. It can be seen that the results obtained with the $k-\varepsilon$ Monin-Obukhov turbulence model agree very well with the experiment at more than 50% of the test sections.

Table 2
Comparative analysis of five turbulent models with the experimental model in the test sections

	Test sections	$k-\varepsilon$ RNG	$k-\varepsilon$ std	$k-\varepsilon$ realizable	$k-\varepsilon$ std MO	$k-\varepsilon$ std ABL
Velocity distribution	13	-	2	-	6	5
Turbulent kinetic energy	7	-	2	-	4	1
Total	20	-	4	-	10	7

5. Grid dependence test

For the $k-\varepsilon$ variant which performed better in our test, using the reference mesh, a grid dependence test was performed in order to see the necessary refinement threshold over which the solution become unchanged.

A number of additional 3 meshes were used, using the same meshing technique as for the reference grid, with a total number of cells equal to 6588, 105408 (refined \times 1) and 421632 (refined \times 2) cells, respectively.

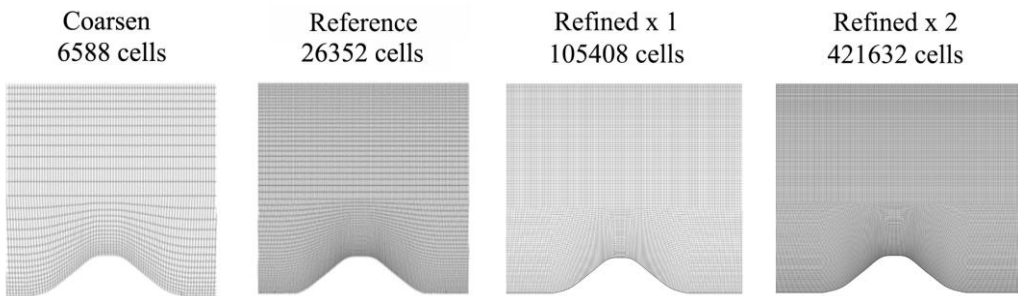


Figure 6. Coarse mesh, standard mesh and refine solution meshes.

Comparisons were made in sections of interest L4 and L5 for the turbulent kinetic energy obtained with the $k-\varepsilon$ Monin - Obukhov turbulence model on coarsen and finer meshes (see Fig. 7).

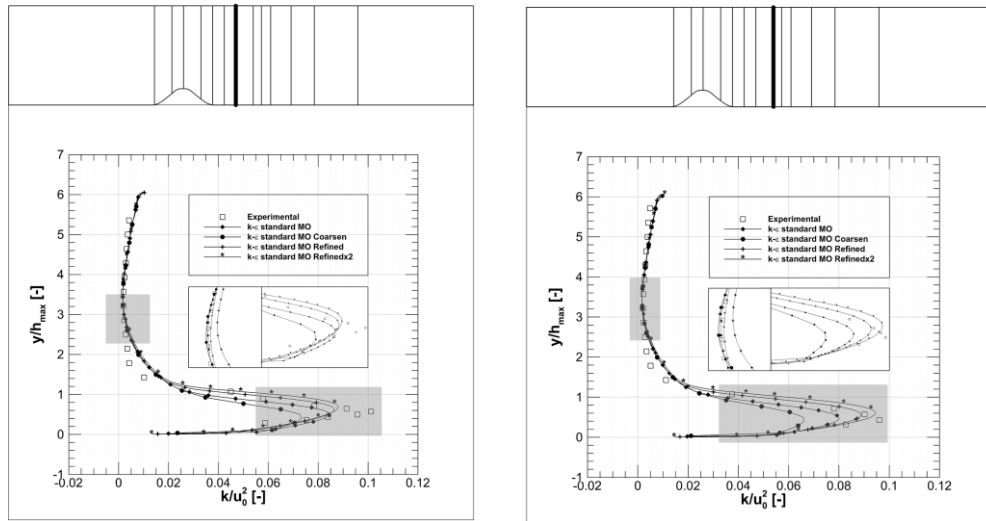


Fig. 7. Distributions of dimensionless turbulent kinetic energy k/U_0^2 depending on the vertical distance y/h_{max} obtained with the Monin - Obukhov turbulence model on different meshes compared with the experimental distributions in section L4 and L5, downstream of the hill.

The comparative analysis reveals that the best results are obtained on the mesh refined two-times with respect to the standard mesh.

6. Conclusions

We performed numerical simulations on the flow over a 2D polynomial surface in ANSYS Fluent expert software, comparing the results with the experimental tests conducted by Almeida et al. using accurate Laser Doppler measurements within a fully developed turbulent channel flow.

We have tested 6 different turbulence models based on the $k-\varepsilon$ model i.e. standard, realizable, RNG, Monin - Obukhov and ABL model using a standard grid that reproduces the flow domain.

Comparisons of velocity and turbulent kinetic energy distributions showed that the $k-\varepsilon$ Monin-Obukhov turbulence model leads to numerical results that agree the best with experimental measurements.

Several meshes were tested, in order to establish the solution dependence with the grid. Coarser and finer computational grids were tested with the $k-\varepsilon$

Monin-Obukhov turbulence model. The purpose was to see which grid leads to numerical results that agree well with the experiment while the numerical simulations remain cost-effective in terms of computational resources. It was found that the optimum grid is the one that is refined two times with respect to the standard one.

R E F E R E N C E S

- [1]. *G. P. Almeida, D. F. G. Durao and M. V. Heitor*, "Wake flows behind two dimensional model hills", *Exp. Thermal and Fluid Science*, **vol. 7**(1), 87-101, 1992.
- [2]. *G. P. Almeida, D. F. G. Durao, J. P. Simoes and M. V. Heitor*, "Laser-Doppler measurements of fully developed turbulent channel flow", *Proc. 5th Symp. Appl. Laser Techniques to Fluid Meet*, 5-12, 1992.
- [3]. *W. H. Snyder, and J. C. R. Hunt*, "Experiments on stably and neutrally stratified flow over a model three-dimensional hill", *Journal of Fluids Mechanics*, **vol. 96**, 671-704, 1980.
- [4]. *J. P. Castro and A. Haque*, "The structure of a turbulent shear layer bounding a separation region", *Journal of Fluid Mechanics*, **vol. 179**, 439-468, 1987.
- [5]. *J. Ch. Bonnin, T. Buchal and W. Rodi*, "ERCOFTAC Workshop on data bases and testing of calculation methods for turbulent flows", *ERCOFTAC Bulletin*, 48-54, 1995.
- [6]. *** ERCOFTAC Classic Database. Available at: <http://cfd.mace.manchester.ac.uk/> [Accessed 2013].
- [7]. *D. Cabezon, J. Sumner, B. Garcia, J.S. Rodrigo and C. Masson*, "RANS simulations of wind flow at the Bolund experiment", *EWEA 2011 - European Wind Energy Conference & Exhibition*, 141-144, 2011.